

COMPARISON OF DATA CLASSIFICATION TECHNIQUES APPLIED TO TLS POINT CLOUDS

A. Guarnieri^a, A. Vettore^a, F. Pirotti^a, M. Marani^b

^a CIRGEO – Interdepartment Research Center for Geomatics, University of Padova,
viale dell'Università 16, 35020 Legnaro (PD), Italy - cirgeo@unipd.it

^b IMAGE - Department of Hydraulic, Maritime, Environmental and Geotechnical Engineering,
University of Padova, via Loredan 20, 35131 Padova, Italy - marani@idra.unipd.it

Commission V, WG V/3

KEY WORDS: Terrestrial Laser Scanner, DTM, data clustering, salt-marsh, ecogeomorphic dynamics

ABSTRACT

Marshes are ubiquitous landforms in estuaries and lagoons, where important hydrological, morphological and ecological processes take place. These areas attenuate sea action on the coast and act as sediment trapping zones. Due to their ecosystem functions and effects on coastal stabilization, marshes are crucial structures in tidal environments, both biologically and geomorphologically, and fundamental elements in wetland restoration or coastal realignment schemes. Observational fluvial geomorphology has greatly benefited in the last decades from the wide availability of digital terrain data obtained by orthophotos and by means of accurate airborne laser scanner data (LiDAR). On the contrary, the spatially-distributed study of the geomorphology of intertidal areas, such as tidal flats and marshes, remains problematic owing to the small relief characterizing such environments, often of the order of a few tens of centimetres. Here, we present the results of the application of terrestrial laser scanning (TLS) for the generation of a DTM of the bare soil within a tidal marsh in the Venice lagoon. To this aim, different procedures for clustering of TLS data have been investigated. Post-processing of the very high resolution data obtained shows that the laser returns coming from the low vegetation present (about 0.3-1.0m high) can be satisfactorily separated from those coming from the marsh surface, allowing to generate detailed DSM and DTM. Furthermore, the DTM is shown to provide unprecedented characterizations of marsh morphology, e.g. regarding the cross-sectional properties of small-scale tidal creeks (widths of the order of 10cm), previously observable only through conventional topographic surveys, thus not allowing a fully distributed description of their morphology.

1. INTRODUCTION

Since its first appearance onto the scene in 1998, terrestrial laser scanning (TLS) has been used for a variety of applications like structural monitoring, cultural heritage recording, transportation related surveys, landslide mapping, tunnel surface inspection, forensic and damage assessment. The dense and accurate recording of surface points has promoted the research towards the development of automated or semi-automated methods for feature extraction, object recognition and object reconstruction. A further research field, which could potentially benefit from the use of TLS data deals with the study and modelling of salt-marsh ecogeomorphological patterns in intertidal environments. The goal of these studies is the development of predictive models of ecological and morphological co-evolution of such areas. Tidal marshes are transition zones between marine and terrestrial systems playing an important role in the geomorphological and biological dynamics of intertidal areas (Marani et al., 2006). Marshes attenuate sea action on the coast and act as sediment trapping zones. Due to their ecosystem functions and effects on coastal stabilization, marshes are crucial structures in tidal environments, both biologically and geomorphologically, and fundamental elements in wetland restoration or coastal realignment schemes. In spite of this important role, the understanding of salt-marsh dynamics still lacks a comprehensive and predictive theory, mainly because many of the linkages between the relevant ecological and geomorphological processes are poorly understood. The study of ecogeomorphic dynamics is complicated by the fact that the processes shaping the biological and geomorphological characters of a salt marsh occur over a wide range of spatial scales, from few centimetres to several kilometres. While the role of large scale features (e.g. the large tidal channels through

which water, sediment and nutrient exchanges between a tidal environment and the sea take place) is quite obvious, it is worthwhile to emphasise that also small-scale geomorphic features (e.g. within the centimeter to one meter range) are very important in the morphological and ecological evolution of the system. A fundamental problem in intertidal studies is to observationally identify the relationship between terrain morphology, ground elevation, and the spatial distribution of vegetation species, in order to clarify the complex ecogeomorphological processes governing the temporal evolution of tidal environments (Marani et al., 2007). Observational fluvial geomorphology has greatly benefited in the last decades from the wide availability of digital terrain data obtained by orthophotos and remote sensing data (Belluco et al., 2006) and by means of accurate airborne LiDAR data (Wang et al., 2008). On the contrary, the spatially-distributed study of the geomorphology of intertidal areas, such as tidal flats and marshes, remains problematic owing to the small relief characterizing such environments, often of the order of a few tens of centimetres.

In this paper we present the results of the application of TLS technology for the generation of a DTM of the bare soil within a tidal marsh in the Venice lagoon. Several classification methods (both supervised and unsupervised) were applied to the aligned scans in order to separate the laser returns coming from the low vegetation present (about 0.3-1.0 m high) from those coming from the marsh surface. The aim of this task is to derive high resolution DTMs of salt-marshes. This is important in ecogeomorphic studies of intertidal environments, where conventional LiDAR technologies cannot easily separate first and last laser returns (because of the low vegetation height) and thus provide models of the surface as well as of the terrain. Results of the high resolution data post-processing show that the

laser returns coming from the low vegetation present (about 0.5-1.0 m high) can be satisfactorily separated from those coming from the marsh surface, allowing to generate detailed DSM and DTM. Furthermore, the DTM is shown to provide unprecedented characterizations of marsh morphology, e.g. regarding the cross-sectional properties of small-scale tidal creeks (widths of the order of 10 cm), previously observable only through conventional surveying methods, thus not allowing a fully distributed description of their morphology. The remainder of the paper is organized as follows. In section 2 an overview of the test area is presented, while the survey methodology is described in section 3. We then present the details of our approach for laser data classification, along with achieved results, in section 4. We finally conclude the paper in section 5 with a short discussion.

2. THE STUDY SITE

The Lagoon of Venice (Figure 1a), located in north-east Italy, is a water body with a surface of about 550 km² and an average depth of approximately 1.1 m, characterized by a semidiurnal tide with a range of about of about ± 0.7 m above mean sea level (hereinafter amsl). It is connected with the Adriatic sea by three inlets and receives freshwater inputs from a few tributaries, contributing a quite small water flux, but a relatively large associated input of solutes (e.g. nutrients from agricultural areas). The Lagoon as a whole is currently experiencing a transformation towards a marine system with important environmental implications. Though the general trend is quite clear, the mechanisms shaping the landscape of the Lagoon, as for many other tidal environments, are not well understood and, while some of its parts experience intense erosion, some salt-marshes are actually accreting. Thus salt-marshes of the Venice lagoon represent a key element to understand the dynamics of such intertidal environment.

The study site is located within an artificial salt marsh in the Venice lagoon (Figure 1b), a microtidal area of great environmental importance. Because of anthropogenic causes, the extent of intertidal morphological structures has been steadily decreasing during the past century. The marsh surface, in particular, shrank from 149 km² in 1912 to just 47 km² in 1997 and to 37 km² in 2003. Such a degradation proved particularly intense in the southern part of the lagoon, where the artificial marsh examined here is located (Figure. 1a,b). The “Ministero delle Infrastrutture – Magistrato alle Acque di Venezia – through “Consorzio Venezia Nuova” started reconstructing the marsh in 1992, and has monitored it since its completion. The marsh, which is characterized by a surface of about 30 ha and an average elevation of 0.60 m amsl, is constituted by sediment obtained from dredging the tidal channels in proximity of the Chioggia inlet. Because of the resulting relatively high level of the platform, four lower areas were created by dredging in 1998 together with six tidal channels connecting them to the rest of the lagoon. One of these lower-lying areas is studied here (Figure. 1b,c) and is characterized by a surface of about 3500 m², with a nearly constant elevation of 0.15 m amsl. The site is almost completely surrounded by high levees (1 m amsl) and is connected to the rest of the platform by an artificial tidal channel. The boundary levees isolate the site from the surrounding marsh, providing well defined boundary conditions for modelling purposes. Moreover, because of the high elevation of the artificial marsh, water reaches the study area almost exclusively through the artificial channel connecting it downstream (i.e. in the direction of the ebb tide) to the lagoon and upstream to another low-lying area (Figure 1b). In previous

studies, changes in the morphological features of the site were monitored through remote sensing and field surveys which provided useful direct observations and ground ancillary information.

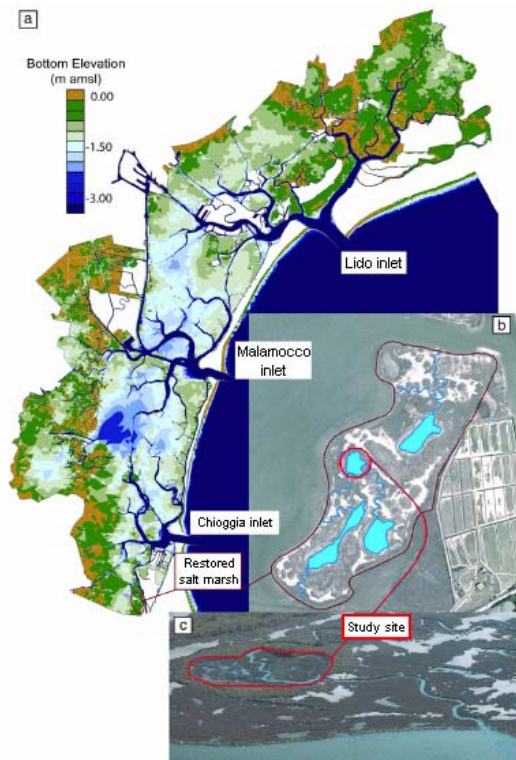


Figure 1. a) Map of the Venice lagoon and location of the artificial marsh. b) Artificial marsh located in the southern lagoon. The lower-lying areas and the artificial channels are also depicted. c) Aerial view of the study site. The high boundary levees surrounding the site are highlighted.

3. DATA COLLECTION

As described in (Axelsson, 1999), airborne LiDAR technology is ideally well suited for measuring topography in marsh environments. Indeed, in a sparse vegetation area laser pulses can at least partly penetrate through the vegetation cover, thus some returns come from the ground, which, if correctly identified, can be separated from vegetation points to map the ground underneath. However, it is not a simple task to determine which laser returns are actually ground returns, especially in the case of salt-marsh areas, characterized by a relatively short but dense canopy. The effective use of airborne LiDAR measurements in tidal environments requires addressing two main challenges: a) vegetation and ground returns cannot be easily separated by using first and last echoes because of the limited height of vegetation, compared with the duration and temporal separation of the laser pulses. As a consequence, the first and last returns of LiDAR data coincide; b) accurate determination of ground elevation requires the removal of the laser echoes reflected by the canopy or by other above-ground objects. However, marsh areas are covered by dense vegetation covering underlying terrain features, and are typically incised by a complex network of small channels with low elevation relief. This leads to a relatively low chance of laser penetration through marsh vegetation.

In order to overcome such issues in our study area (where vegetation height was ranging between 20 and 70 cm, see

Figure 2), we surveyed the salt marsh with a Leica HDS 3000 terrestrial laser scanner. Measurements were performed during low tide period to avoid interferences due to water on the marsh surface. To minimize shadowing effects due to the tilting of the laser beam (especially in the channel network), the scanner was mounted on a aluminium custom-built tripod 3 m above the marsh surface (Figure 3).



Figure 2. Vegetation of the test area.



Figure 3. The tripod used to rise up the laser scanner.

Working in a marshy and often muddy area, all the equipment has been configured in order to be completely dismantled and packed for easy transportation by car and boat.

The marsh, about 100m x 150m, was fully surveyed from just 2 stations placed in opposite positions in order to get a uniform as possible terrain sampling. Setting a scan resolution of 5 cm, a total amount of about 3 million points was acquired, with an average measurement density of 200 points/m². In order to validate and compare the results of the different classification methods, two subsequent GPS surveys were performed. In the first one, positions of 8 retroreflective targets (Figure 4) were measured with a double-frequency Leica GPS receiver in fast-static mode. GPS data were then differentially corrected with a reference station located in the nearby (about 4 km far from the study site) achieving an average accuracy of about 2cm for the target coordinates. The same targets were also surveyed with the laser scanner with higher accuracy (2mm) than the rest of the area. Such artificial targets were required in order to get easily detectable features to be used as matching points for scan registration. Indeed, given the inherent unstructured nature of marsh areas, no particular geometric features are commonly available for this operation. In the second survey about 470

points were measured in RTK mode along the salt marsh. Achieved point elevations (ellipsoidal heights) were then used in the data processing step to validate the various DTMs derived by the classification methods applied to the laser elevations (Z coordinates), as described in next section.



Figure 4. A subset of the retroreflective targets.

4. DATA PROCESSING

The whole data processing stage was subdivided in three different steps, detailed in the following sub-sections: a) scan registration, b) model georeferencing and c) data classification.

4.1 Scan registration

At the end of each main scan, 8 sub-scans were run from Cyclone software in order to automatically detect the center of the retroreflective targets. Thanks to this strategy, the scan registration could be accomplished in easy and fast way, saving a lot of processing time. Actually we needed to perform twice this operation as in a first run we did not obtained satisfactory results in terms of residual RMS error on aligned target coordinates. Thus in a second attempt, 6 out of the 8 targets were selected according to the lower residual error achieved in the previous run. In this way the RMS registration error could be cut down from 12mm to 7mm. The resulting whole aligned point cloud is shown in figure 5, where measured points are rendered according to the RGB data provided by the laser scanner built-in CCD camera.

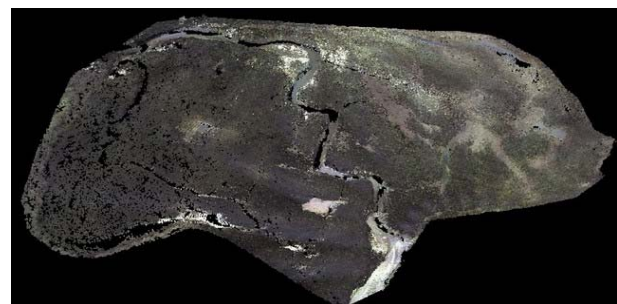


Figure 5. The aligned point cloud rendered with RGB data.

4.2 Model georeferencing

Once aligned, the 3D model of the study area and the GPS measurements had to be referenced in the same frame in order to validate the DTMs, generated by data clustering, with elevations (ellipsoidal heights) of GPS points. In order to avoid the computational issues related to the use of great numbers, as typically occur when dealing with mapping frames, we transformed the GPS coordinates from the WGS84 Datum to the laser scanner reference frame. Indeed, we were interested in determining the capability of a TLS, such as the Leica HDS

3000, to penetrate the low vegetation of salt marshes and to recover the surface of the underlying bare soil. It was therefore not needed to relate the point cloud to an absolute mapping frame: data processing could be done even working on a local (i.e. laser scanner) frame. Parameters required for the reference frame transformation were derived by manually matching the laser coordinates of the 6 retroreflective targets used for scan registration with the coordinates of corresponding GPS points measured in fast-static mode. After this step we achieved a residual RMS error of 2.3cm, which we considered enough satisfactory for our purposes. Then a 7 parameter transformation was applied to the RTK-GPS data in order to co-register the GPS levelling with the aligned pointcloud. Figure 6 shows the two datasets overlaid each other: here, out of the 470 GPS measurements only the subset covering the area of interest is displayed.

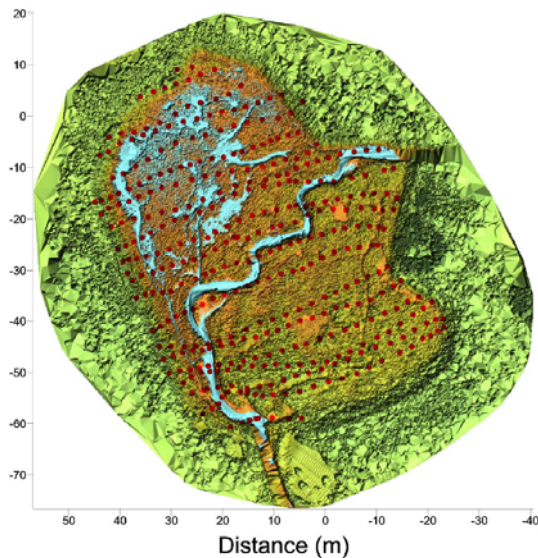


Figure 6. GPS levelling overlaid onto the TLS 3D model.

4.3 Data classification

As mentioned in the introductory section of this paper, the study and modelling of salt-marsh ecogeomorphological patterns in intertidal environments represent a prerequisite for the development of predictive models of ecological and morphological co-evolution of such areas. The comprehension of the complex eco-morphological processes governing the temporal evolution of tidal environments requires to clearly identify the relationship between terrain morphology, ground elevation, and the spatial distribution of vegetation species. Thus, the generation of accurate models of the bare terrain (i.e. DTMs) is of primary importance. On the other hand, the presence on salt marshes of a low vegetation, ranging between 20-30cm and 70cm, makes this task very challenging. Terrestrial laser scanners can ideally solve for such issue given the small size of the laser beam, which is commonly limited to a few millimeters up to a distance of some hundreds of meters. Compared to airborne LiDAR, TLS provides a better capability to penetrate low and dense vegetation, though its lower productivity would limit the extent of the surveyed area per unit of time.

In this section we describe the procedure applied to the aligned 3D model, derived by TLS measurements, in order to automatically separate the laser returns coming from the low vegetation from those coming from the marsh surface. Basically, three different filtering methods (both supervised and

unsupervised) were applied: minimum elevation, K-means and Gaussian Maximum Likelihood Estimate (GMLE).

In a first attempt we also tried to use a different approach based on multispectral data only (i.e. Intensity and the RGB data), in a similar manner as described in (Lichti, 2005). However, rapid changes in light conditions, as commonly occurs when capturing panoramic views in outdoor environments, affected the quality of digital images acquired by the laser built-in CCD camera. The presence of high dynamics (too dark or too bright images) prevented us from achieving satisfactory results with multispectral data.

The analysis was carried out on two different sub-areas of the study site, featuring dense and sparse vegetation (Figure 7). For each dataset a DTM was generated by a classification method, according to the following scheme:

- 1) Minimum elevation (Z coordinate);
- 2) Minimum elevation + K-means;
- 3) Minimum elevation + Maximum likelihood;
- 4) K-means;
- 5) K-means + Minimum elevation;
- 6) Maximum likelihood;
- 7) Maximum likelihood + Minimum elevation.

Such scheme was designed in order to evaluate the effectiveness of the classification based on laser elevation with respect to supervised and supervised methods, based on the Intensity data only.



Figure 7. The dense (left) and sparse (right) vegetation areas.

Prior to apply those clustering methods to laser measurements, a preliminary data gridding operation was performed in order to reduce the model resolution. Indeed, for eco-geomorphological studies DTMs with the same high resolution of the TLS 3D model (200 pts/m²) are not necessary, therefore the laser model can be downsampled saving computational time. A further and major advantage of this operation relies on the fact that a DTM can be derived, whose points more likely belong to the ground rather than to the vegetation canopy. Indeed, taking into account the limited size of the laser beam, it is quite reasonable to think that as the cell size increases, laser returns reflected by the canopy can be better filtered out, getting a DTM mainly composed of ground points. In order to choose the optimal cell size for gridding both the dense and the sparse vegetation area, we applied the method described in (Wang et al., 2008). Basically, we assumed the lowest laser elevation value within a small size area to be due to a ground reflection. The extent of the small area over which the lowest elevation value of TLS records coincides with the actual ground elevation was determined using a large number of ground survey points as follows. The occurrence of true ground hits in a sample of laser measurements is a random variable. To estimate the sample size required to obtain at least one ground hit we performed a

statistical analysis. Each RTK-GPS measurement was considered as a reference observation and the related elevation value was compared to the elevation of surrounding TLS points falling within search circles with increasing radius R ($R = 0.2, 0.4, 0.6, \dots, 2m$), centered at the GPS survey point. For each laser point and value of R , the return characterized by the smallest Z_{laser} value was identified and compared to the 'actual' elevation value, Z_{GPS} . When all GPS reference observations were considered, a scatter plot of GPS measurements vs. Z_{laser} elevations was produced for each circle radius (see Figure 8). For the smallest circle ($R = 0.2m$) almost all echoes come from the canopy and TLS estimates tend to be greater than GPS observations. As the circle radius is increased, the probability of the laser beam being reflected by the ground surface also increases and the 'optimal' radius can be selected as the smallest radius giving rise to the best match between TLS and RTK-GPS measurements.

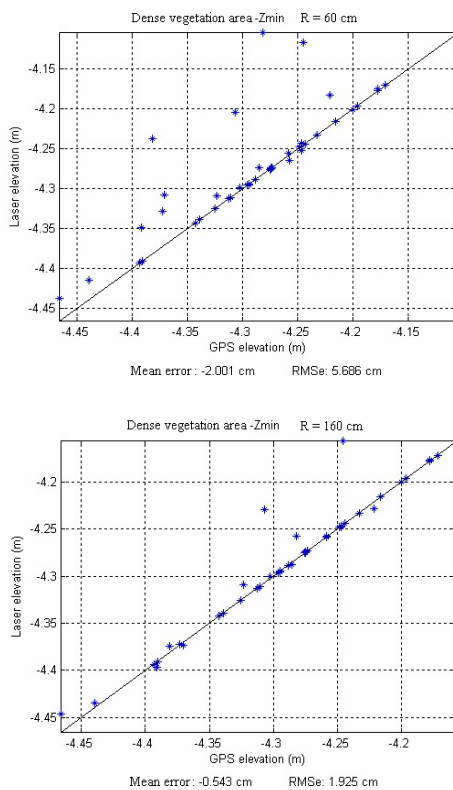


Figure 8. Scatter plot of GPS measurements vs. laser estimates of ground elevation.

The described procedure was applied twice to both selected vegetation areas (dense and sparse): in a first run laser data were compared with a subset of GPS points, selected as Ground Control points, (GCP) then the same procedure was applied to the gridded laser points whose elevation values were compared with the remaining subset of GPS measurements, used as Check points (CP). Out of the original 470 RTK-GPS points, 80 were used as reference observations for the dense vegetation area (50% as GCPs) and 60 points for the sparse vegetation area (50% as GCPs). Figure 9 shows the dependence of the mean and RMS error on the radius chosen to produce the laser estimate of ground elevation. As regards the dense vegetation area, the mean error (blue dots) initially rapidly approaches zero, but appears a roughly constant value when $R > 1.4m$. Conversely, the RMS error (red circles) decreases with increasing radius. Similar remarks can be applied to the sparse

vegetation area, though here the RMS error shows a more constant value when $R > 1.2m$. Note that the maximum difference between a GPS point and the corresponding lowest laser point (as found by the algorithm) lays around -5m and -3m for the dense and the sparse vegetation area respectively. This result confirms the difficulty even for a terrestrial laser scanner to penetrate areas with dense canopy. Laser elevations displayed in figures 8 and 9 have negative values because the direction of the Z axis of the TLS reference frame is pointing upwards. Results achieved from data gridding show that there indeed exists an optimal size for the search neighborhood in which the lowest laser return represents a true ground reflection. In this case, we selected a cell size of 1.6m and of 1.2m respectively for the dense and the sparse vegetation area.

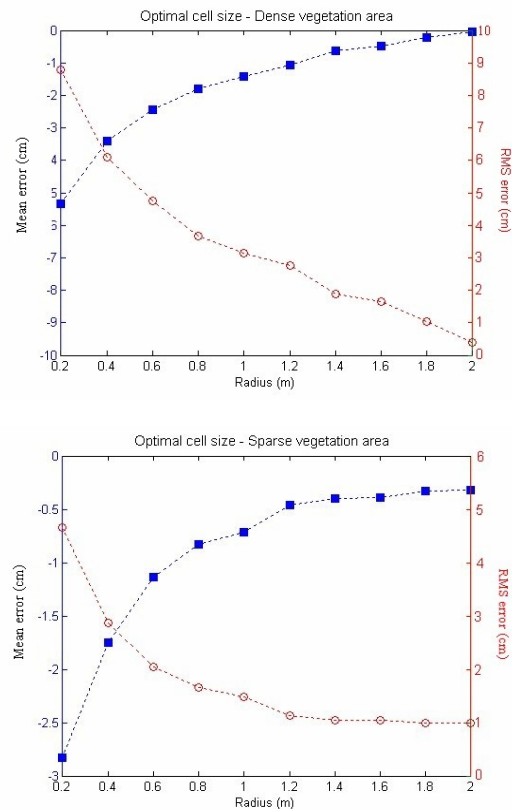


Figure 9. Mean and RMS error of the laser estimation error as functions of the size of the local search neighborhood.

According to the adopted classification scheme, laser data were filtered not only on the basis of elevation values but also by exploiting the spectral information, i.e. the Intensity data. To this aim we applied both supervised (Maximum Likelihood) and unsupervised (k-means) clustering methods, commonly used in the field of Remote Sensing. Such methods were applied both separately and in combination with the minimum elevation algorithm. For each test we discriminated between three classes: vegetation, soil and water. The latter was introduced to account for the presence of water in a few areas along the main artificial channel crossing the marsh. However, for the generation of the DTMs, the classes soil and water were grouped together. As regards the Maximum Likelihood classification method, the required training sets were manually extracted from the whole 3D model of the salt marsh as shown in figure 10. It should be noted that samples extracted to estimate the training parameters for the vegetation class were not optimal, as the operator could not correctly separate laser returns due to vegetation from the ones coming from the soil below.

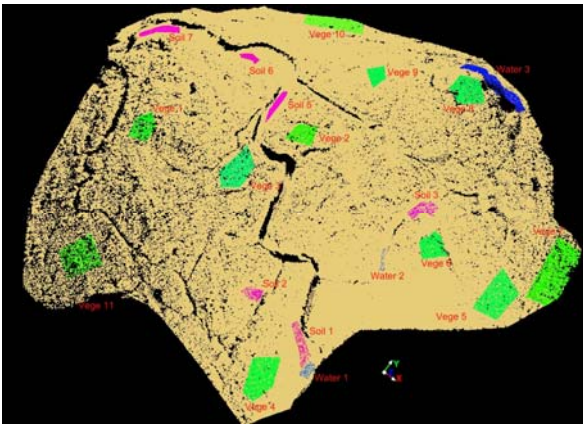


Figure 10. Training sets for the Maximum Likelihood estimate. Vegetation samples are depicted in green, soil samples in purple and water samples in blue.

Results achieved from the data classification step are summarized in tables 1 and 2 for the dense and sparse vegetation area respectively.

Filter \ Radius	60 cm		80 cm		160 cm	
	Mean error (cm)	RMSe (cm)	Mean error (cm)	RMSe (cm)	Mean error (cm)	RMSe (cm)
Z min	-2.001	4.686	-1.443	3.749	-0.543	1.925
Z min + K-means	-1.432	3.134	-0.866	2.562	-0.133	0.978
Z min + Max. Likelihood	-1.443	3.349	-0.665	2.127	-0.146	0.788
K-means	-9.319 (mean error)		14.062 (RMSe)			
K-means + Z min	-2.196	5.121	-1.406	3.880	-0.285	1.055
Max. Likelihood	-7.651 (mean error)		12.913 (RMSe)			
Max. Likelihood + Z min	-2.594	5.025	-1.394	3.358	-0.230	1.052

Table 1. Results of data classification applied to the dense vegetation area.

Filter \ Radius	60 cm		80 cm		120 cm	
	Mean error (cm)	RMSe (cm)	Mean error (cm)	RMSe (cm)	Mean error (cm)	RMSe (cm)
Z min	-1.142	2.354	-0.768	1.596	-0.521	1.225
Z min + K-means	-0.505	1.212	-0.303	0.892	-0.119	0.490
Z min + Max. Likelihood	-0.496	1.186	-0.225	0.656	-0.102	0.390
K-means	-6.506 (mean error)		9.896 (RMSe)			
K-means + Z min	-1.143	2.354	-0.769	1.596	-0.224	0.991
Max. Likelihood	-6.362 (mean error)		9.570 (RMSe)			
Max. Likelihood + Z min	-1.129	2.346	-0.771	1.594	-0.215	0.982

Table 2. Results of data classification applied to the sparse vegetation area.

Both tables show that the best results, in terms of mean and RMS error, were achieved with the classification based on the minimum elevation concept, while minor improvements were added with the cascade application of the k-means or the Maximum Likelihood Estimator, i.e. with the methods based on spectral data only. A similar result holds if we consider the

inverse procedure based on the application of either spectral data clustering method followed by the minimum elevation filtering. However in this case, the decreases of the mean and RMS error are not as pronounced as in the first approach, though of the same level of magnitude. Looking at both tables it is also clear that the application of a classification algorithm based only on spectral data (i.e laser Intensity) does not provide satisfactory results, maybe because Intensity and elevation data are not strictly related: spectral spatial distribution are basically independent each other. All these remarks hold for both tested vegetation sub-areas.

5. CONCLUSIONS

In this paper we have presented the results of the application of TLS technology for the generation of a DTM of the bare soil within a tidal marsh in the Venice lagoon. Three different clustering methods were applied to acquired scans in order to separate the laser returns coming from the low vegetation present (about 0.3-1.0 m high) from those coming from the marsh surface. Results of data post-processing showed that the most effective classification procedure is the one based on the cascade application of minimum elevation filtering followed by a clustering based on spectral information (i.e. reflected laser Intensity). Moreover, it can be shown that derived DTMs provide unprecedented characterizations of marsh morphology, e.g. regarding the cross-sectional properties of small-scale tidal creeks (widths of the order of 10 cm), previously observable only through conventional surveying methods, which not allow for a fully distributed description of their morphology

References

- Axelsson, P., 1999. Processing of laser scanner data algorithms and applications, *ISPRS Journal of Photogrammetry & Remote Sensing*, vol. 54, pp. 138-147.
- Belluco, E., Camuffo, M., Ferrari, S., Modenese, L., Silvestri, S., Marani, A., Marani, M., 2006. Mapping salt-marsh vegetation by multispectral and hyperspectral remote sensing. *Remote Sensing of Environment*, 105, 54- 67.
- Guarnieri, A., Brusco, N., Cortelazzo, G.M., Vettore, A., 2007. Automatic 3D modeling with multi-spectral textures and classical ICP-based approach: a comparison. *Proceedings of 8th Conference on "Optical 3D Measurement Techniques"*, Zuerich, Switzerland, 9-12 July.
- Lichti D. D., 2005. Spectral filtering and classification of terrestrial laser scanner point clouds. *The Photogrammetric Record*, Volume 20, Number 111, pp. 218-240(23).
- Marani, M., Silvestri, S., Belluco E., Ursino, N., Comerlati, A., Tosatto, O., 2006. Spatial organization and ecohydrological interactions in oxygenlimited vegetation ecosystems. *Water Resources Research*, 42, W06D06.
- Marani, M., D'Alpaos, A., Lanzoni, S., Carniello, L., Rinaldo, A., 2007. Biologically-controlled multiple equilibria of tidal landforms and the fate of the Venice lagoon. *Geophys. Res. Lett.*, 34, L11402.
- Wang C., Menenti M., Stoll M., Feola A., Belluco E., Marani M., 2008. Separation of ground and low vegetation signatures in LiDAR measurements of salt-marsh environments. In review.